

**Zeitschrift:** Eclogae Geologicae Helvetiae  
**Herausgeber:** Schweizerische Geologische Gesellschaft  
**Band:** 89 (1996)  
**Heft:** 1

**Artikel:** Triassic pegmatites in the Mesoizoic middle crust of the Southern Alps (Italy) : fluid inclusions, radiometric dating and tectonic implications  
**Autor:** Sanders, Carlo A.E. / Bertotti, Giovanni / Tommasini, Simone  
**DOI:** <https://doi.org/10.5169/seals-167911>

### **Nutzungsbedingungen**

Die ETH-Bibliothek ist die Anbieterin der digitalisierten Zeitschriften auf E-Periodica. Sie besitzt keine Urheberrechte an den Zeitschriften und ist nicht verantwortlich für deren Inhalte. Die Rechte liegen in der Regel bei den Herausgebern beziehungsweise den externen Rechteinhabern. Das Veröffentlichen von Bildern in Print- und Online-Publikationen sowie auf Social Media-Kanälen oder Webseiten ist nur mit vorheriger Genehmigung der Rechteinhaber erlaubt. [Mehr erfahren](#)

### **Conditions d'utilisation**

L'ETH Library est le fournisseur des revues numérisées. Elle ne détient aucun droit d'auteur sur les revues et n'est pas responsable de leur contenu. En règle générale, les droits sont détenus par les éditeurs ou les détenteurs de droits externes. La reproduction d'images dans des publications imprimées ou en ligne ainsi que sur des canaux de médias sociaux ou des sites web n'est autorisée qu'avec l'accord préalable des détenteurs des droits. [En savoir plus](#)

### **Terms of use**

The ETH Library is the provider of the digitised journals. It does not own any copyrights to the journals and is not responsible for their content. The rights usually lie with the publishers or the external rights holders. Publishing images in print and online publications, as well as on social media channels or websites, is only permitted with the prior consent of the rights holders. [Find out more](#)

**Download PDF:** 21.03.2026

**ETH-Bibliothek Zürich, E-Periodica, <https://www.e-periodica.ch>**

# Triassic pegmatites in the Mesozoic middle crust of the Southern Alps (Italy): Fluid inclusions, radiometric dating and tectonic implications

CARLO A.E. SANDERS<sup>1</sup>, GIOVANNI BERTOTTI<sup>1</sup>, SIMONE TOMMASINI<sup>1, 2</sup>,  
GARETH R. DAVIES<sup>1</sup> & JAN R. WIJBRANS<sup>1</sup>

*Key words:* Southern Alps, rifting processes, thermal evolution, P-T-t paths, pegmatites

## ABSTRACT

The schists in the northern part of the South-Alpine crystalline basement along Lake Como record Barrovian syn-kinematic metamorphism of Variscan age. They cooled below the Rb-Sr whole rock closing temperature at ca. 300 Ma and were exhumed by ca. 6–7 km before the Late Permian. In the Middle Triassic a thermal perturbation affected the South-Alpine middle crust leading to the widespread transformation of garnets into biotite + sillimanite aggregates under static conditions. Anatectic pegmatites were emplaced roughly contemporaneous with the peak temperature conditions. Rb-Sr mineral ages on pegmatites, schists and marbles between 229 and 194 Ma show the crust was again cooling during the Late Triassic, when continental rifting started. Stretching leading eventually to the opening of the Ligurian-Piemont ocean continued until Middle Jurassic times. Fluid inclusion data from the pegmatites establish that only limited decompression took place during Late Triassic to Early Cretaceous cooling. As a result of Alpine shortening, the rocks were eventually exhumed to the surface.

## RIASSUNTO

Dopo aver subito un metamorfismo sin-cinematico di età ercinica, gli scisti del basamento cristallino delle Alpi meridionali affioranti lungo il Lago di Como, furono raffreddati al di sotto della temperatura di chiusura del sistema Rb-Sr per roccia totale a 300 Ma. In un tempo mal definito ma comunque precedente il Permiano superiore essi furono sollevati di 6–7 km. Durante il Trias medio una forte perturbazione termica interessò la crosta inferiore e media delle Alpi meridionali e causò la trasformazione statica del granato in aggregati biotite + sillimanite. Pegmatiti anatectiche furono messe in posto durante il picco termico. Le età radiometriche con il metodo Rb-Sr per vari minerali delle pegmatiti, degli scisti e dei marmi della zona hanno valori compresi tra 229 e 194 milioni di anni fa dimostrando che la crosta stesse raffreddandosi durante il Trias superiore quindi durante il rifting continentale che porterà nel Giurassico medio all'apertura dell'oceano ligure-piemontese. Le inclusioni fluide delle pegmatiti dimostrano che il raffreddamento non fu accompagnato da sollevamento fin quando, con l'inizio dell'orogenesi alpina, le rocce della regione considerata vennero sollevate definitivamente e portate alla superficie.

## Introduction

The crystalline basement of the central and western Southern Alps underwent major deformation and metamorphism during the Variscan orogeny and, starting in the Norian (at

---

<sup>1</sup> Institute of Earth Sciences, Free University, De Boelelaan 1085, NL-1081-HV Amsterdam

<sup>2</sup> Present address: Facoltà di Agraria, Università di Firenze, Piazzale delle Cascine 15, I-50144 Firenze

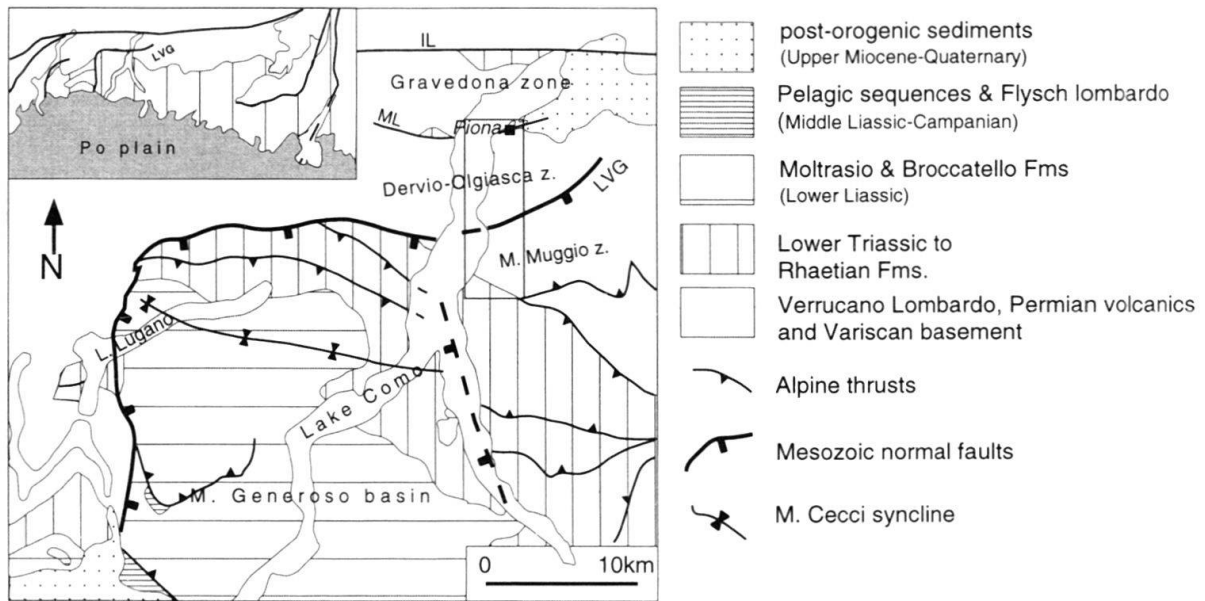


Fig. 1. Schematic geological map of the Lake Lugano-Lake Como area. The northern part of the M. Generoso basin and of its substratum inclusive the Lugano-Val Grande normal fault have been steepened in Alpine times around the M. Cecci syncline. The box along Lake Como corresponds to the Alpine steepened Mesozoic crustal section the lowest part of which contains the pegmatites. LVG = Lugano-Val Grande fault, IL = Insubric Line, ML = Musso Line.

For the inset: thick solid lines correspond to major tectonic features, white areas are crystalline basement, vertical shading indicates pre-Tertiary sediments.

around 215 Ma according to the time scale by Gradstein et al. 1994), was extended in association with the formation of the Adriatic passive continental margin (Bertotti et al. 1993a). From the Late Cretaceous, or later, the Southern Alps were involved in Alpine shortening (Doglioni & Bosellini 1989). A section of the Mesozoic upper to middle crust of Adria is exposed in northern Italy, in the Lake Como area (Fig. 1, 2). In the deepest exposed crustal levels, a swarm of pegmatites is found (Reposi 1914).

In this paper we report a new investigation of the middle crust metamorphic rocks and associated pegmatites. Petrographic observations, fluid inclusion studies and Rb-Sr isotope data enable us to revise some of the existing hypotheses and to reconstruct a detailed tectonic and metamorphic evolution of the South-Alpine middle crust from the Variscan to the Alpine orogenies.

The knowledge of the tectonic history of the Southern Alps after the Variscan orogeny and prior to the Mesozoic extension is incomplete. The South-Alpine crust and large areas of Europe were affected by intense magmatism during the Late Carboniferous to Late Permian (e.g. Bonin et al. 1993, Gebauer 1993). However, there is no general agreement on the tectonic framework during this magmatic activity. In other parts of the Variscan chain, for example the Massif Central (Echtler & Malavieille 1990) and the Black Forest (Eisbacher et al. 1989), magmatism was associated with important extensional and strike-slip faults which have been attributed both to the continental-scale wrenching between Africa and Fennoscandia (Ziegler 1988) and post-collisional extension of the

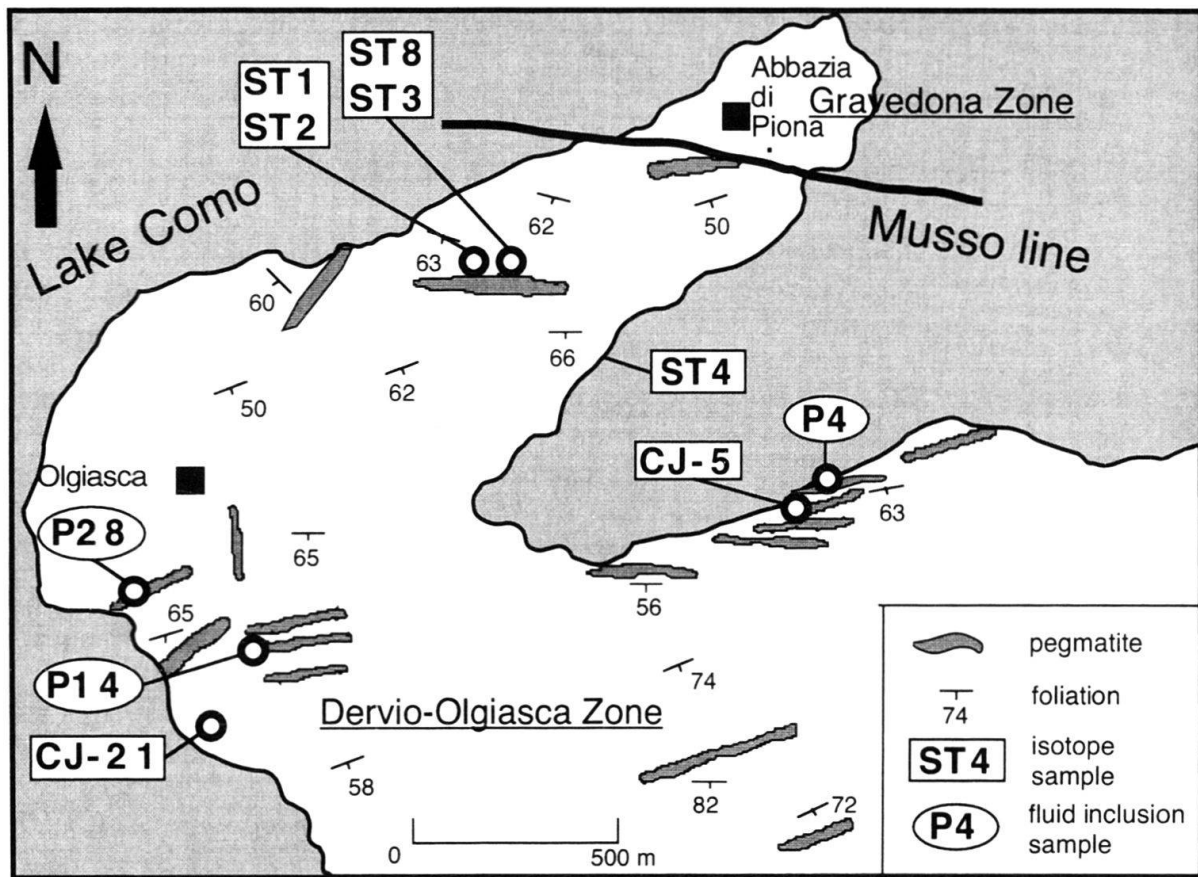


Fig. 2. Geologic map of the Piona area in the northern sector of lake Como (see Fig. 1). The size of the pegmatites has been exaggerated for clarity. Compiled from Reposi (1914), El Tahlawi (1965) and own data.

Variscan chain (e.g. Malavieille 1993); an interplay between the two is obviously possible.

On the basis of the South-Alpine case study, we also want to address the relations between rifting and magmatism (e.g. Wilson 1993). The evidence of the Lake Como section demonstrates that an important thermal anomaly was present in the South-Alpine middle crust before the onset of normal faulting and that it began to cool when the Norian to Liassic rifting started.

### The Lake Como crustal section

The metamorphic basement of the central Southern Alps outcropping between the Insubric line in the north and the sedimentary cover in the south, was formed during pre-Late Carboniferous orogenies. The presently exposed units were metamorphosed under greenschist to amphibolite facies conditions (Borioni et al. 1974). Subsequently, the basement was affected by tectono-thermal events in Permian to Jurassic times and finally involved in Alpine shortening which caused merely a brittle deformation in the outcropping units.

In the northern Lake Como area, the metamorphic basement is subdivided into two main Alpine tectonic units separated by the E-W striking Musso Line (Fig. 1). The Al-

pine unit south of the Musso line, inclusive of the Dervio-Olgiasca and M. Muggio zones, represents an essentially continuous segment of Mesozoic upper to middle crust steepened and exhumed in Alpine times (Bertotti et al. 1993b). Progressively deeper crustal levels are exposed from south to north. In the southern part of the section, the Permo-Triassic sedimentary cover lies stratigraphically on Variscan basement which has undergone no high temperature deformation following regional metamorphism (M. Muggio zone; El Tahlawi 1965). Towards the north, this basement section is interrupted by the Val Grande fault zone, a 700 m thick band of mylonites, ultramylonites and cataclasites which has been interpreted as a deeper part of the Mesozoic Lugano normal fault passively steepened during Alpine shortening (Bertotti 1990, 1991). The Lugano-Val Grande fault juxtaposes the M. Muggio zone in the south with the middle crustal Dervio-Olgiasca zone in the north. The Dervio-Olgiasca zone is made up of a succession of schists and gneisses which show a gradational trend to higher metamorphic grade from south to north (El Tahlawi 1965, Bocchio et al. 1980). The Dervio-Olgiasca zone is limited to the north by the Alpine Musso line. The Alpine unit north of the Musso line is the Gravedona zone and represents a portion of Mesozoic upper crust preserving its Variscan paragenesis (Bocchio et al. 1980) and its Permo-Mesozoic stratigraphic cover (Fumasoli 1974).

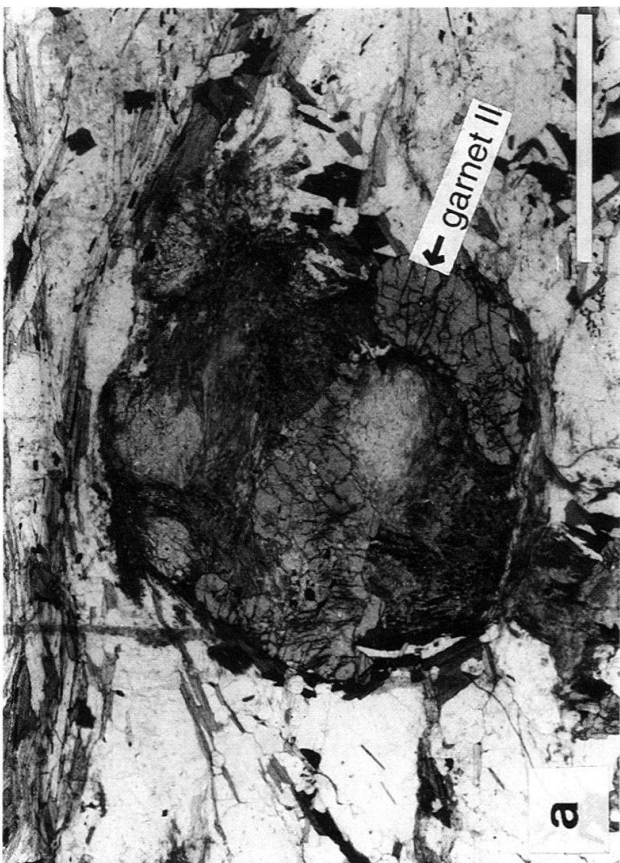
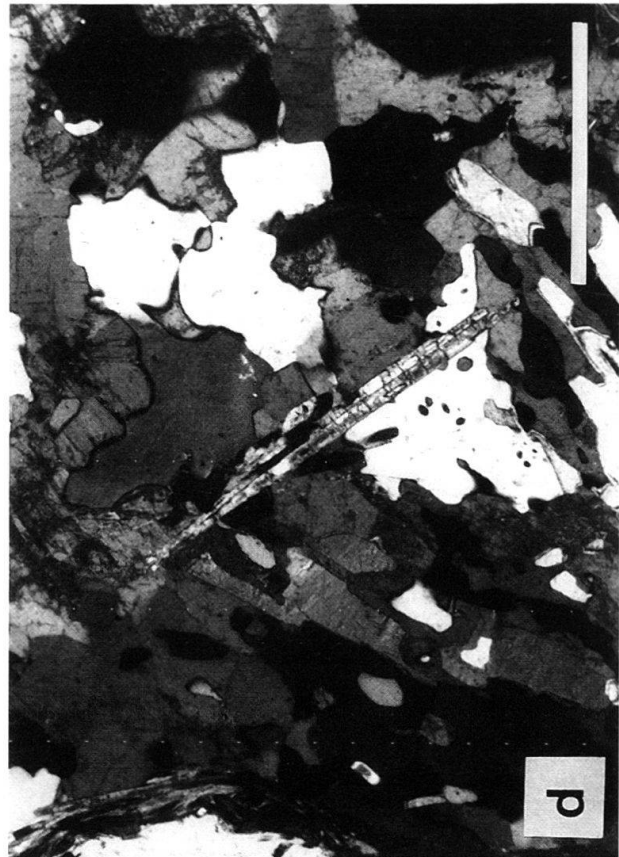
The Piona peninsula, where the pegmatites are found, is part of the Dervio-Olgiasca zone and is the deepest part of the Mesozoic crust exposed in the Lake Como section (Fig. 1). During the Triassic and Jurassic it was situated at a depth of 15–16 km (Bertotti et al. 1993b). Following the work of El Tahlawi (1965), recent petrographic and structural investigations have been conducted in the Lake Como basement (Mottana et al. 1985, 1990, Siletto et al. 1990, Diella et al. 1992, Bertotti et al. 1993b). These studies, however, did not concentrate explicitly either on the pegmatites found in the area or on their host-rock which are used here to provide new information on the Permian to Triassic tectonic evolution of the area.

## The middle crustal rocks of Piona

### *Metamorphic rocks*

The dominant lithology of the Piona region is sillimanite-garnet-mica schist. The schists are relatively coarse-grained and show a clear muscovite and biotite foliation ( $S_1$ ) (El

- 
- Fig. 3. Micrographs of schists and pegmatites from the Piona peninsula. a) "Atoll" garnet in the Piona schists: the central part is composed of a Sill+Bt aggregate pseudomorphically replacing garnet (I). Along parts of the rim a fresh garnet (II) is observed. The overall shape of the older garnet is well preserved pointing to the absence of deformation during the development of the Sill + Bt aggregate. Note the asymmetric pressure shadows which developed during syn- $P_1$  deformation. Sample 21, parallel nichols, bar = 5 mm.
- b) Piona schists. Asymmetric clast of feldspar and garnet, the latter being statically replaced by Sill+Bt. The shape of the clast clearly indicates deformation during a first phase. The undisturbed character of the fibrolite needles and their irregular orientation point to static condition during and after their formation. Sample 30, parallel nichols, bar = 3 mm.
- c) Piona schists. Fibrolite needles growing randomly over the older, first phase fabric. Sample 34, crossed nichols, bar = 1.5 mm.
- d) Sillimanite crystal in one of the Piona pegmatites. Sample 14, crossed nichols, bar = 1 mm.



Tahlawi 1965, Bocchio et al. 1980, Diella et al. 1992). Dm-thick felsic horizons alternate with the more mica-rich parts. The foliation generally dips steeply to the south (Fig. 2) and, in the more micaceous parts, is often wavy and undulated around mm- to cm-sized blasts. Locally, a distinct second schistosity is observed which is defined by a similar mineral assemblage.

The mineralogical assemblage of the Piona schists is mainly formed by a coarse-grained, roughly equigranular matrix with quartz (30%), feldspar (mostly albite-oligoclase, 25%), red-brown biotite (25%), muscovite (15%) and garnet (5%) enclosing large porphyroblastic aggregates of sillimanite/fibrolite, biotite and garnet (Fig. 3a, b) (El Tahlawi 1965, Mottana et al. 1990, Diella et al. 1992). Quartz occurs as a mosaic of unstrained grains in elongated lenses and shows no preferred lattice orientation. Feldspar is internally unstrained, flat and elongated parallel to the main foliation. Biotite crystals can be fresh or partly replaced by fibrolite and sillimanite. The micas, typically 2–3 mm, are often intergrown with quartz and feldspar. Perfectly preserved, up to millimetres long sillimanite occurs as needles that cross-cut the main foliation, the porphyroblastic aggregates and the boundaries between schists and pegmatites. The distribution of the sillimanite is very heterogeneous throughout the rock. The porphyroblastic aggregates consist of intergrowths of fibrolitic and prismatic sillimanite and biotite, and often have rims of new garnet resulting in an atoll-like structure (Fig. 3a) (Mottana et al. 1990). Smaller, euhedral garnets are common in some sections. Locally, chlorite and sericite are found which probably developed in the last evolutionary stages.

The oldest paragenesis (P1) is formed by  $Qtz + Pl + Grt(I) + Bt(I) + Ms$  and indicates amphibolite facies conditions. The P1 paragenesis was syn-kinematic as shown by the asymmetric shadow zones associated with the larger crystals or aggregates (Fig. 3a, b) and by the alignment of micas along the foliation.

A younger paragenesis P2 is characterized by sillimanite-biotite (II) aggregates pseudomorphically replacing garnet (I) porphyroblasts (c.f. Yardley 1977) and by the growth of fibrolite and millimetres-long sillimanite needles. The fresh biotite crystals found in the matrix of the rock could also be associated with the P2 paragenesis, but they could also be related to P1 and have escaped the reaction to sillimanite (c.f. Yardley 1977). It cannot be distinguished whether biotite (II) and sillimanite grew simultaneously, or if garnet was solely replaced by biotite (II) in first instance, followed by nucleation of sillimanite from the biotite (Yardley 1977). Renewed growth of garnet took place in a late stage of P2 and formed fresh garnet rims around the aggregates. Regrowth was probably also associated with nucleation and growth of small euhedral garnets in the matrix over P1 textures (Fig. 3a). We see no evidence for major deformation associated with the development of the P2 mineral assemblage. This interpretation is mainly based on the perfect preservation of the sillimanite-biotite aggregates which are delicate features and would clearly be disrupted by a deformation event (Fig. 3a, b). Additionally, the long fibrolite needles are often radially oriented and undeformed (Fig. 3c). Local preferred orientation is mostly related to overgrowth of older anisotropies. The minor displacement bands that locally occur associated with mainly sillimanite have no regional significance.

The youngest paragenesis P3 is made up of minor chlorite and sericite formed along localized shear bands possibly contemporaneous with the formation of the rare non-annealed mylonitic quartz bands found in the Piona peninsula.

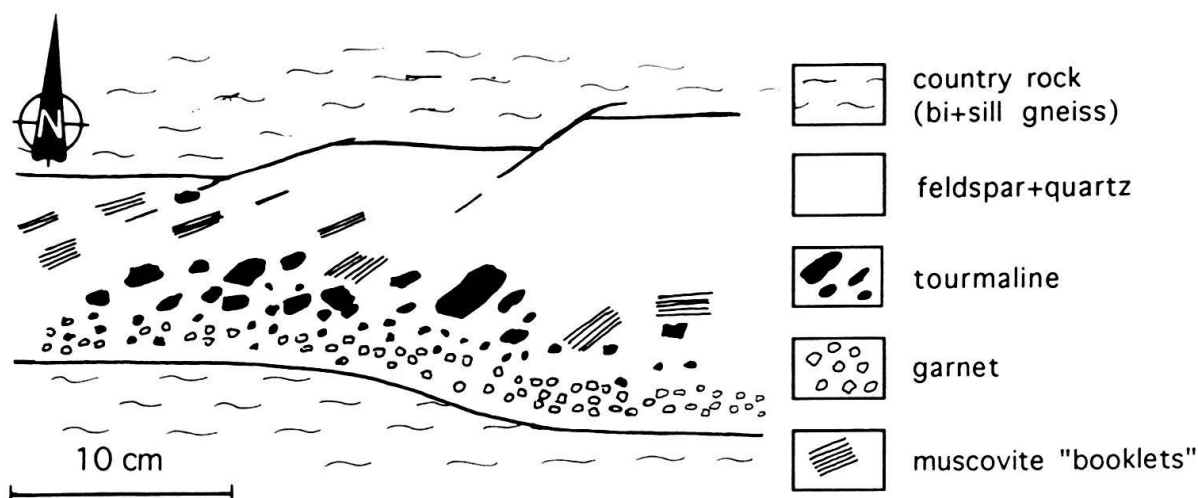


Fig. 4. Sketch from photograph of a pegmatite. Both country-rock foliation and pegmatites are sub-vertical. Note the asymmetric layering in the pegmatite. Its position during emplacement can be deduced restoring for Alpine tilting, i.e. rotating the foliation and the pegmatite back to horizontal along a E-W axis in a clockwise sense locking west. The southern part of the pegmatite becomes thereby its upper part.

### *The pegmatites*

A swarm of about 30 pegmatitic dykes is found in the Piona peninsula and on the northern flank of M. Legnoncino (El Tahlawi 1965) (Fig. 2). The pegmatites are generally tabular or lens-shaped and usually several decimetres thick and up to tens of metres long. They are typically not folded, record limited brittle deformation and are generally concordant or slightly discordant to the main foliation. Offshoots of the pegmatites are sometimes observed. The intrusive contacts with the country rock are usually sharp, but in some cases they are transitional with the host-schists enriched in micas, garnets and tourmalines.

The pegmatites have little mineralogical variations suggesting that they belong to one single genetic group and that they have a similar age (El Tahlawi 1965). All contain anhedral grey-transparent quartz (ca. 30%), microcline K-feldspar (ca. 20%), albite/oligoclase (ca. 25%) and muscovite (ca. 15%). The most common phases among the accessories are small euhedral garnets and black tourmaline; the latter forms well developed intergrowths with quartz and plagioclase. Much rarer are biotite and chlorite. Quartz, feldspar and some mica have irregular and notchy grain boundaries ascribed to initial rapid pegmatite solidification. The grain size varies between mm and several cm. Grains in each pegmatite, however, tend to have limited size variations. A layered arrangement of the minerals parallel to the pegmatite walls is frequently observed. In a few cases, the pattern is clearly asymmetric with garnets concentrated and tourmaline becoming finer-grained towards the southern margin (Fig. 4). Since the pegmatites are pre-Alpine (see below), their present-day position has to be corrected for Alpine south-ward tilting. Once this is done, the southern margin becomes the roof of the pegmatite. Since garnet has a higher density than most of the surrounding minerals, its enrichment in the upper part of the

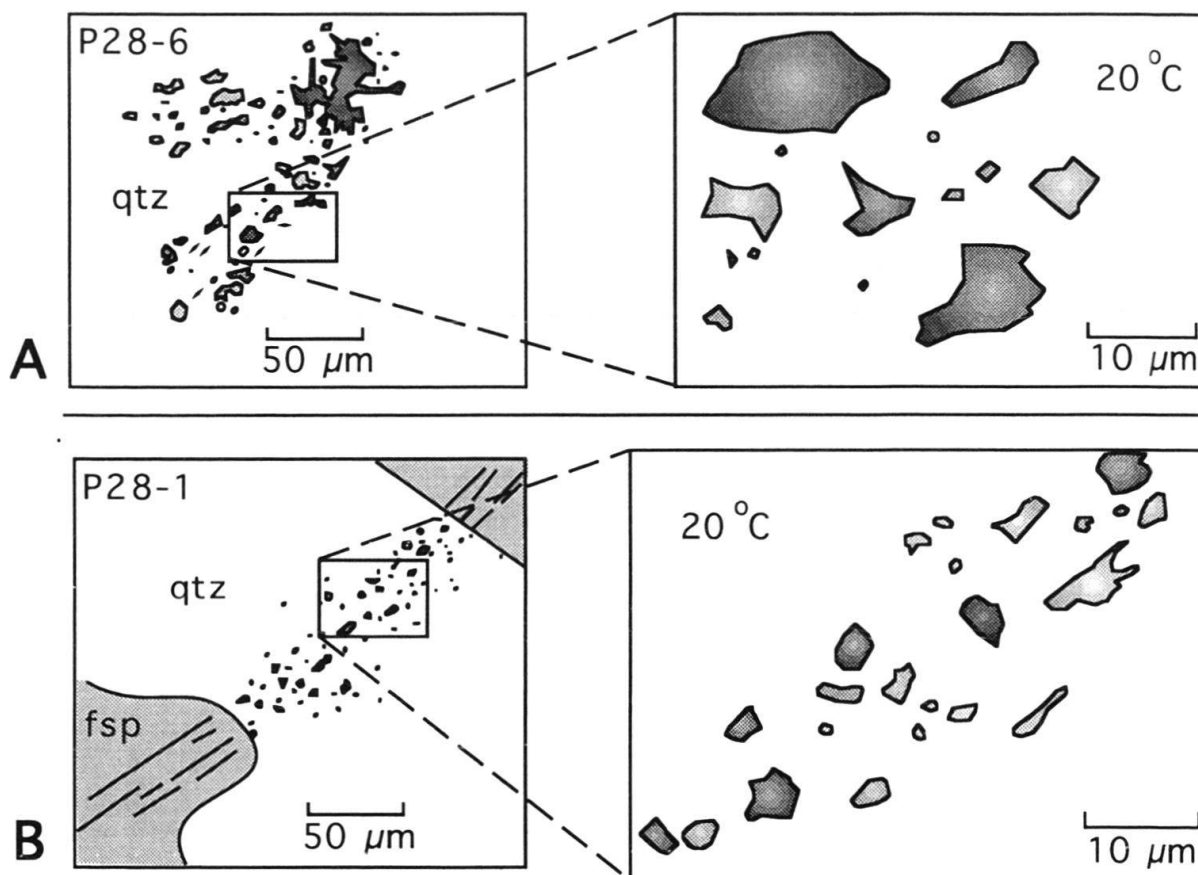


Fig. 5. Sketches of A) primary (P28-6) and B) secondary (P28-1) inclusions at room temperature.

A) The exploded primary inclusion is visible in the upper part of the left diagram and is surrounded by the randomly oriented daughter inclusions.

B) The secondary inclusions in quartz lie on a trail which crosses mineral boundaries.

pegmatite cannot be explained by gravitational processes in the melt phase (e.g. Jahns 1982).

The pegmatites suffered very little deformation. Microscopic ductile deformation features are restricted to slightly undulose quartz, very limited quartz sub-grain rotation along micro-faults, and kink-bands in feldspar and muscovite. Fracturing is in some cases common but displacements are negligible.

Metamorphic minerals are rare, but can be used to link the intrusions to the metamorphic events. Fibrolitic intergrowth and prismatic sillimanite blasts overgrowing the pegmatite are documented in some sections (Fig. 3d). This demonstrates that the pegmatites formed before or during the initial stages of the P2 metamorphism in the country rock. In a few cases, sericite is found replacing feldspars or filling voids.

The mineralogical association of the pegmatites closely corresponds to low-T minima melts in the system  $Ab + An + Or + Qtz + H_2O$ , and suggests an anatectic origin of the pegmatites by melting of a pelitic protolith. This is supported by the simple qualitative and quantitative mineral content, the high Al contents and the large amount of carbon ( $CO_2$ ,  $CH_4$ ) in the decrepitated primary fluid inclusions (see below) which is probably de-

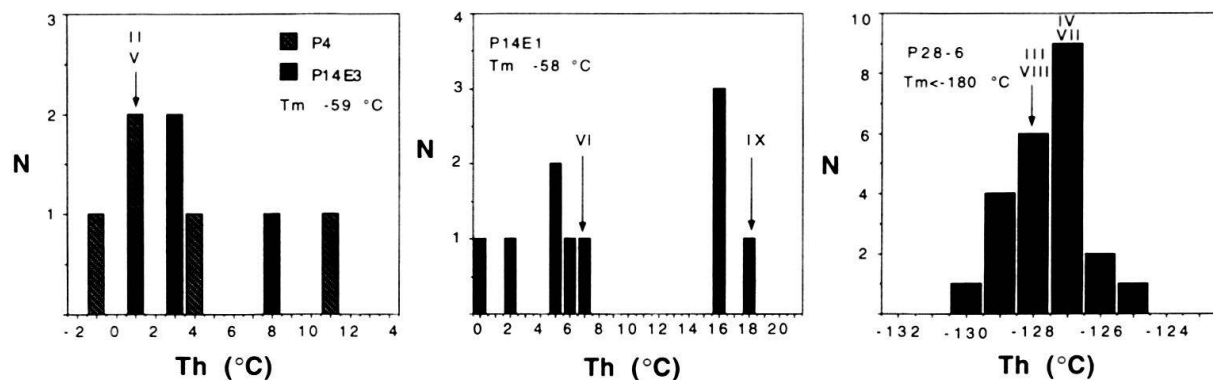


Fig. 6. Microthermometry histograms for the daughter inclusions. The roman numbers refer to the inclusion selected for RAMAN analysis. Th = homogenization temperature L-V(L), Tm = final melting temperature of CO<sub>2</sub>. Total N = 41. Note the different scales in the three diagrams.

rived from organic matter available in the pelitic schists (personal communication J. Touret 1993). Mottana et al. (1990) and Diella et al. (1992) report evidence of local incipient melting in the country rocks. An origin by fractionation of differentiated allochthonous granites is unlikely because of the general lack of rare element minerals.

#### *Fluid inclusions in the pegmatite*

Both decrepitated primary inclusions and secondary inclusions have been found in quartz crystals of the Piona pegmatites. About 65% of them are H<sub>2</sub>O-rich (brines), 25% are gas-rich (usually a binary combination out of CO<sub>2</sub>, N<sub>2</sub> and CH<sub>4</sub>), and the remaining 10% are empty or contain vapor. Brine inclusions are found only as secondary inclusions.

*Decrepitated primary inclusions* (essentially gas-rich). Primary inclusions in the pegmatites are formed by fluids trapped in cavities during the crystallization of host minerals in the melt. They can be identified because they are relatively large, have an irregular shape, occur isolated and randomly distributed throughout the thin section (Roedder 1984). The densities of these fluids, represented by the isochore line, record the P-T conditions at the moment of consolidation. All primary inclusions in the Piona pegmatites have undergone explosion in a late stage. The released fluids are trapped in clusters of daughter inclusions (Roedder 1984). The decrepitated primary inclusions are very irregular, more or less radial-shaped and are surrounded by a cluster of smaller inclusions. Primary and decrepitated primary inclusions in the Piona pegmatites are only of the gaseous type. The size of the central (exploded) inclusions ranges from 30 to 60  $\mu\text{m}$  (see Fig. 5a). The various tails starting from the very irregular central inclusions suggest an original smaller size which is estimated between 20–40  $\mu\text{m}$ . The surrounding daughter inclusions show a great variety in sizes from < 1  $\mu\text{m}$  to 15  $\mu\text{m}$ . As expected in the case of explosion, the decrepitated primary inclusions show the same phase changes upon cooling as the daughter inclusions, but could not be measured precisely because of poor visibility. The clouds of daughter inclusions were measured for microthermometry (Fig. 6) and show homogeneous phase ratios. Inclusion compositions were determined by RAMAN analyses (Table 1) and the densities are calculated according to Holloway & Reese (1974), van

Tab. 1. RAMAN analyses of gaseous inclusions; all data are mean values. Molar volumes (in ccm) in column A are according to Holloway & Reese (1974) and van den Kerkhof (1988); in column B according to Thiery et al. (1994). Note how values in column B are accordance but slightly higher than those of column A. HHC = reaction to higher hydrocarbons.

| sample:incl. | Th(L-V(L) (°C) | CO <sub>2</sub><br>(mole%) | N <sub>2</sub> (mole%) | CH <sub>4</sub><br>(mole%) | remarks         | molar volume<br>A | molar volume<br>B |
|--------------|----------------|----------------------------|------------------------|----------------------------|-----------------|-------------------|-------------------|
| P28-1:I      | -39.9          | 61                         | 39                     | --                         |                 | 44                | 47                |
| P4:II        | 1.1            | 87                         | 13                     | traces                     |                 | 52                | 55                |
| P28-6:III    | -128.3         | --                         | 63                     | 37                         |                 | 54                |                   |
| P28-6:IV     | -126.8         | --                         | 61                     | 39                         |                 | 54                |                   |
| P14E3:V      | 0.6            | 73                         | 25                     | 2                          |                 | 60                | 65                |
| P14E1:VI     | 6.8            | 79                         | 19                     | 2                          |                 | 61                | 63                |
| P28-6:VII    | -127.5         | --                         | 71                     | 29                         | reaction to HHC | 62                |                   |
| P28-6:VIII   | -128.2         | --                         | 73                     | 27                         |                 | 62                |                   |
| P14E1:IX     | 17.5           | 87                         | 13                     | --                         | traces HHC      | 70                | 80                |
| P28-2        | -127           | 24                         | 46                     | 30                         | metastable      |                   |                   |

den Kerkhof (1988) and Thiery et al. (1994); the resulting isochores are shown in Figure 10.

*Secondary inclusions* are formed by fluids entering cracks which are subsequently annealed. Since cracks can form during the entire post-consolidation history of the pegmatites, the densities of the trapped fluids record conditions at some stage during the rock evolution. Secondary inclusions occur in trails of approximately equally-sized inclusions with homogeneous phase ratios. All secondary inclusions observed in the Piona pegmatites are too small (< 3 µm) for microthermometry measurements. An exception is the gaseous trail P28-1 (Fig. 5b) with inclusions up to 8–10 µm and a calculated molar volume of 44 ccm (Fig. 7 and Tab. 1) (Holloway & Reese 1974, van den Kerkhof 1988).

Secondary brine inclusion trails generally contain three phases at room temperature and have very homogeneous phase ratios with less than 5% vapor (degree of fill), cubic solid crystals (halite) indicating a total amount of 30 to 40% wt NaCl, and the liquid which is presumably (NaCl) salt saturated water. Final melting temperatures ranging from –25 to –43 °C and the presence of a second cubic mineral suggest significant Ca contents. Inclusions with mixtures of gases and brines are very rare. Gaseous and brine inclusions are generally found in distinct domains. The absence of mixed inclusions means that the two fluids, although both possibly present in the melt, were immiscible at the time of trapping and subsequently operated as two separate systems.

### **Rb-Sr dating: implications for pegmatite emplacement age and for cooling history**

Rb-Sr mineral ages are useful to decipher the temperature evolution of the middle crust. Unfortunately, there are only few, widely scattered Sr isotope data for the South-Alpine basement east of Lake Lugano (Hanson et al. 1966). As a consequence, the age of the pegmatite emplacement and thus the tectonic context during emplacement has been de-

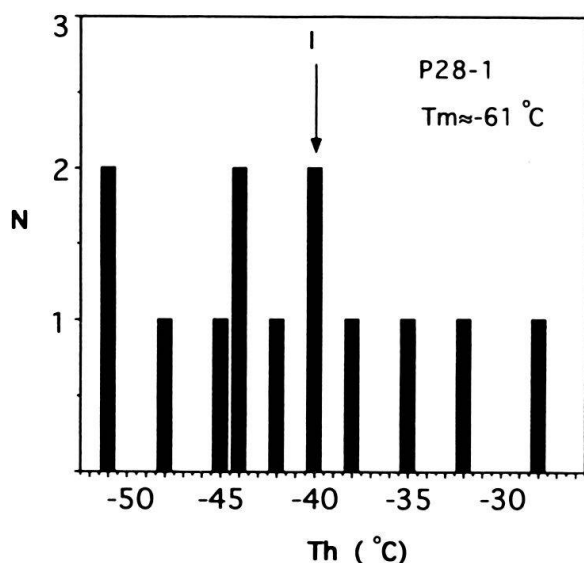


Fig. 7. Microthermometry histogram of the trail of secondary inclusions P28-1. Roman number refers to the inclusions selected for RAMAN analysis. Th = homogenization temperature L-V(L), Tm = final melting temperature of CO<sub>2</sub>. Total N = 13.

bated (e.g. Hanson et al. 1966, Ferrara & Innocenti 1974, Bertotti et al. 1993b). We have therefore carried out new Sr isotope analyses on minerals from the different rock types of the Piona Peninsula.

Isotope analyses were performed at the Radiogenic Isotope Laboratory of the Vrije Universiteit of Amsterdam (NL). Mineral separation was achieved through routine separation techniques (e.g. fall table, magnetic separator) on 300–400  $\mu$  grain fraction. Before analysis each mineral aliquot was carefully screened and hand picked, resulting in a sample purity > 99% for all minerals except biotite which may contain some apatite, zircon and oxides. Approximately 100 mg of biotite and 50–30 mg of plagioclase and muscovite were dissolved in pressurised teflon PFA vials using an HF-HNO<sub>3</sub> mixture. After 3–4 days the sample was evaporated to dryness and was then completely dissolved in hot 6N HCl. Roughly 20% of the solution was spiked using either mixed <sup>87</sup>Rb-<sup>84</sup>Sr (samples ST) or separate <sup>87</sup>Rb and <sup>84</sup>Sr spikes (samples CJ). Rb and Sr were separated using either 6 ml of AG50W  $\times$  8 cation exchange resins or 0.15 ml of SrSpec resins. Total procedure blanks for Rb and Sr were typically < 20 and < 100 pg, respectively. Isotopic ratios were measured on a Finnigan MAT261 thermal ionization mass spectrometer with multiple Faraday collectors. Sr isotope compositions were measured in dynamic mode, and were normalised to <sup>86</sup>Sr/<sup>88</sup>Sr = 0.1194. Uncertainty in Rb/Sr is  $\pm$  1%. The <sup>87</sup>Sr/<sup>66</sup>Sr of NIST SRM987 was  $0.71028 \pm 2$  (N = 15) at the time of data collection.

The results of our Sr isotope analyses are reported in Table 2, divided according to the different lithotypes.

*Pegmatites* – two out of three pegmatites (ST1 and ST8) crop out in the central part of the peninsula (Fig. 2). The K-feldspar-muscovite isochrons yield indistinguishable ages ( $208 \pm 4$  and  $215 \pm 4$ , Tab. 2). The albite-muscovite isochron from the third pegmatite sample (CJ-5) yields an older age ( $224 \pm 6$  and  $229 \pm 7$ , duplicate analyses, Tab. 2).

*Schists* – Two samples (ST2 and ST3) were collected along the contact with pegmatitic bodies. Feldspar-muscovite-biotite from both samples yield well-defined isochrons (MSWD < 1, Tab. 2). The third schist sample (CJ-21, Tab. 2) was collected in the southern part of the peninsula, several tens of meters away from the closest pegmatite. The whole rock-muscovite (in duplicate) yield an “isochron” of ca. 300 Ma, significantly older than the age of the pegmatites. We interpret this as suggesting that the feldspar population of this sample did not equilibrate during the thermal events that, further to the north, caused extensive resetting of mineral ages.

Tab. 2. Results of radiometric dating. Uncertainty in measured  $^{87}\text{Sr}/^{86}\text{Sr}$  refers to least significant digits and represents  $\pm 2$  s run precision. Ages have been determined according to York (1969), errors in ages have been calculated at 95% confidence level.

| lithotype | sample |            | Rb     | Sr     | $^{87}\text{Rb}/^{86}\text{Sr}$ | $^{87}\text{Sr}/^{86}\text{Sr}$ | 2s       | Age (Ma) | MSWD     |
|-----------|--------|------------|--------|--------|---------------------------------|---------------------------------|----------|----------|----------|
|           |        |            | p.p.m. | p.p.m. | atomic                          | atomic                          |          |          |          |
| pegmatite | ST1    | Kfeld      | 33.1   | 173.2  | 0.5547                          | 0.725702                        | $\pm 8$  | 208      | $\pm 4$  |
|           | ST1    | musc       | 463    | 13.44  | 102.8                           | 1.028210                        | $\pm 17$ |          |          |
| pegmatite | ST8    | Kfeld      | 103    | 14.15  | 21.29                           | 0.810255                        | $\pm 14$ | 215      | $\pm 4$  |
|           | ST8    | musc       | 890    | 1.426  | 3948                            | 12.8367                         | $\pm 11$ |          |          |
| pegmatite | CJ-5   | albite 1   | 7.24   | 586.5  | 0.03579                         | 0.728202                        | $\pm 11$ | 224      | $\pm 6$  |
|           | CJ-5   | musc 1     | 138    | 177.9  | 2.245                           | 0.735234                        | $\pm 11$ |          |          |
| pegmatite | CJ-5   | albite 2   | 7.26   | 583.0  | 0.03610                         | 0.728206                        | $\pm 12$ | 229      | $\pm 7$  |
|           | CJ-5   | musc 2     | 125    | 181.5  | 1.998                           | 0.734607                        | $\pm 10$ |          |          |
| schist    | ST3    | pl         | 7.21   | 265.2  | 0.07884                         | 0.724928                        | $\pm 9$  | 213      | $\pm 3$  |
|           | ST3    | musc       | 230    | 27.34  | 24.53                           | 0.799402                        | $\pm 11$ |          |          |
|           | ST3    | biot       | 705    | 2.350  | 1170                            | 4.26171                         | $\pm 9$  |          |          |
| schist    | ST2    | Kfeld      | 53.2   | 148.8  | 1.036                           | 0.733864                        | $\pm 11$ | 194      | $\pm 3$  |
|           | ST2    | musc       | 309    | 34.52  | 26.10                           | 0.802594                        | $\pm 11$ |          |          |
|           | ST2    | biot       | 873    | 1.714  | 2464                            | 7.57395                         | $\pm 12$ |          |          |
| schist    | CJ-21  | wr         | 92.7   | 78.7   | 3.418                           | 0.736989                        | $\pm 11$ | 305      | $\pm 26$ |
|           | CJ-21  | musc 1     | 155    | 93.02  | 4.822                           | 0.743078                        | $\pm 11$ |          |          |
|           | CJ-21  | musc 2     | 155    | 92.33  | 4.858                           | 0.743070                        | $\pm 12$ |          |          |
| marble    | ST4    | calcite    | 0.1393 | 139.1  | 0.002897                        | 0.709257                        | $\pm 10$ | 198      | $\pm 4$  |
|           | ST4    | white mica | 274    | 3.644  | 231.1                           | 1.359854                        | $\pm 23$ |          |          |

*Marble* – The marble sample from the Piona peninsula yields a calcite-white mica age of  $198 \pm 4$  Ma. This age is indistinguishable from the age obtained from the schist sample ST2 and is consistent with the fine-grain size of the marble (i.e. lower closure temperature).

The most relevant result of our measurements is that the Piona pegmatites cooled below the muscovite closing temperature for Rb/Sr in a time span comprised between  $229 \pm 7$  Ma and  $208 \pm 4$ . Given the high closing temperature for Rb/Sr in muscovites ( $550 \pm 50$  °C according to Blanckenburg et al. 1989) we consider these values to be close to the emplacement ages of the pegmatites. With the available results, we are not able to convincingly explain the scatter in the data. The “background” crustal temperature at the depth levels where the pegmatites were emplaced (14–15 km) can be indirectly constrained. The sillimanite needles crossing the pegmatite/country rock boundary and present in the pegmatites themselves, demonstrate that thermal conditions allowing for the formation of sillimanite over the entire Piona area (600–720 °C, Diella et al. 1992) must have been present in the crust during pegmatite emplacement, i.e. at some time around 240–220 Ma. This is consistent with the local anatexis origin of the pegmatites and with the observation of incipient-melting features in the Piona schists (Diella et al.

1992). Ar/Ar measurements on muscovites and biotites from schists and pegmatites of the Piona region provide very well constrained ages between 191 and 200 Ma, thereby demonstrating that by this time, the entire crust had cooled below 350–300 °C (Wijbrans & Bertotti 1994).

With the available data, however, we are not able to describe the detailed thermal evolution of the area between cooling through the Rb/Sr and Ar/Ar closing temperatures for muscovites. The observation that the three point mineral isochrons of the schists have a low MSWD, establishes that at least the schists adjacent to the pegmatites cooled from ca. 650 °C (sillimanite formation) to the closure temperature of biotite (ca. 350 °C, Giletti 1991) on a timescale comparable to the error on the isochron age (few millions of years). If this were not the case micas would have behaved as open systems for Sr and an isochron would not be preserved (Gawen et al. 1995). The mineral ages vary between ca. 227 to 208 Ma for pegmatites and between 213–194 Ma for the schists. Some of the spread in the ages can be explained by the different grain size of the rocks with lower blocking temperatures in finer grained rocks (Dodson 1979). In addition, different modal mineralogy will lead to differences in the effective blocking temperature of the different rock types (Gawen et al. 1995). However, the spread in these ages is hard to reconcile with the inferred rapid cooling recorded by the schist mineral isochrons unless these reflect different local thermal/emplacement events. This would be compatible with the resorption and regrowth features observed in the garnets of the schists (e.g. Mottana et al. 1990).

### **A P-T-t path for the Piona rocks**

According to Diella et al. (1992), the oldest clear metamorphic assemblage recognized in the Dervio-Olgiasca zone is Pl + Bt + Ms + Grt ± Ky and formed at  $T = 500\text{--}650$  °C and  $P = 7\text{--}9$  kbar. Despite the absence of kyanite, we assume that their estimates apply also to the Piona schists because of the structural continuity within the Dervio-Olgiasca zone and because of the proximity with the presumable sample localities. The absence of kyanite from the Piona area is possibly caused by a stronger P2 overprint.

Following peak metamorphic conditions, the Piona rocks first underwent decompression and cooling (e.g. Mottana et al. 1990). Our new isotopic data show that temperatures must have been below the muscovite-albite Rb-Sr closing temperature of ca.  $550 \pm 50$  °C at  $301 \pm 10$  Ma and that, therefore, a clockwise, direct path between P1 and P2 is not allowed. The pressure decrease achieved during this stage is not very well constrained but it could have been of about 2–3 kbar which roughly corresponds to the pressure difference between P1 and P2 determined by Diella et al. (1992) (Fig. 8). In any case, the present day geological setting along Lake Como shows that the Piona rocks were at a depth of ca. 15 km during the late Permian when the Verrucano clastics were deposited. Assuming reasonable rock density values, this also implies that most of the pressure decrease from P1 (7–9 kbar) to P2 (4.5–5.5 kbar) had been achieved already before the end of the Permian.

Post-Variscan cooling and exhumation was interrupted, or, more probably, followed by an important thermal event which led to the P2 metamorphic assemblage. Conditions of formation of the sillimanite-biotite assemblage have been estimated at  $T = 600\text{--}720$  °C and  $P = 4.5\text{--}5.5$  kbar by Diella et al. (1992). These estimates are similar to those obtained

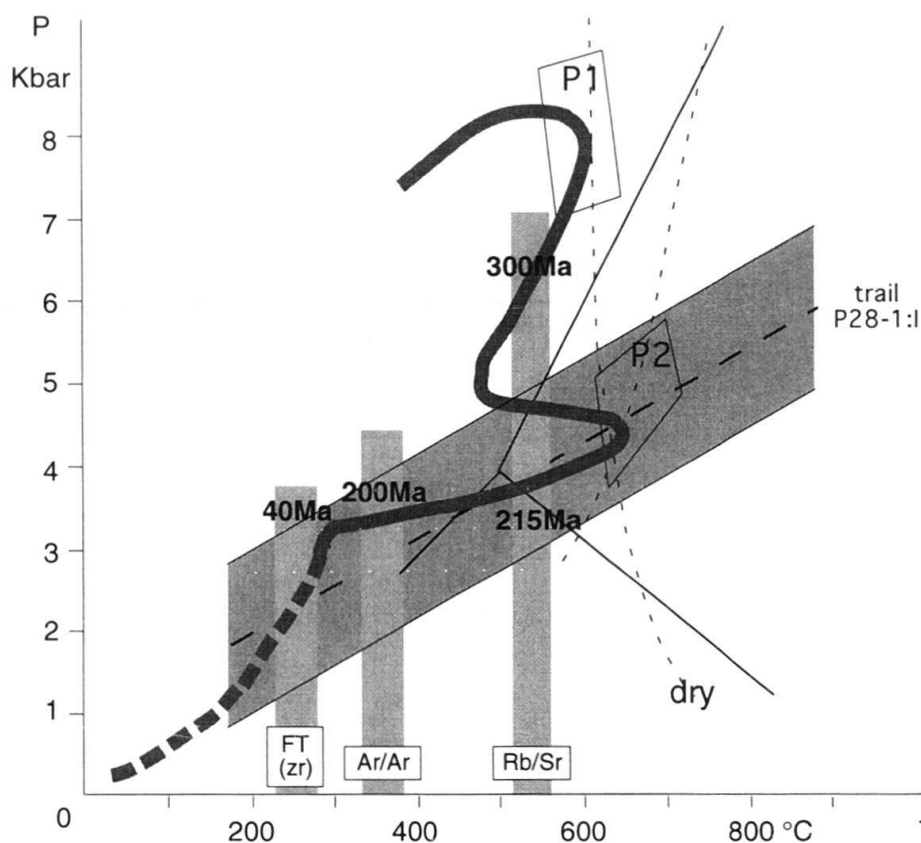


Fig. 8. P-T-t path for the Piona crustal segment. Vertical shaded bars indicate approximate closing temperatures for the Ar/Ar and Rb/Sr isotopic systems and for the fission tracks in zircons. The thick dashed line is the isochore for the secondary inclusions of trail P28-1 which formed when the P-T path crossed the isochore and are not decrepitated. In order to prevent decrepitation the P-T path has to remain within 1kbar from it (shaded bar). Thin dashed curves are the solidus curves for wet and dry pelites (from Thompson & Tracy 1979).

by Mottana et al. (1990) once corrected for the 3–4 km deeper position in the Mesozoic crust of the samples measured by Diella et al. (1992). The middle crustal rocks of the Piona region were therefore heated during the thermal event by at least 200 °C. The similarity between the P conditions determined for the P2 assemblage and those expected at the depth of 14–15 km at which the Piona rocks were lying, implies that heating was essentially isobaric. The post-kinematic texture of the P2 assemblage suggests that no deformation took place during heating.

Our radiometric data are not able to constrain the age at which the thermal anomaly was produced which caused the P2 metamorphism and during which the pegmatites were emplaced. A long duration of the thermal event is, however, unrealistic given the difficulty of preserving a strongly perturbed thermal gradient of about 40–45 °C/km such as the one present in the area during P2 for a long period of time (> few millions of years).

Since the Piona pegmatites were emplaced before or during the early stages of the P2 event (Middle Triassic), we can use their secondary fluid inclusions (trail 28-1 which defines the isochore of Fig. 8) to constrain the P-T evolution after P2. The trail crosses several grains and therefore must have formed after the consolidation of the pegmatite

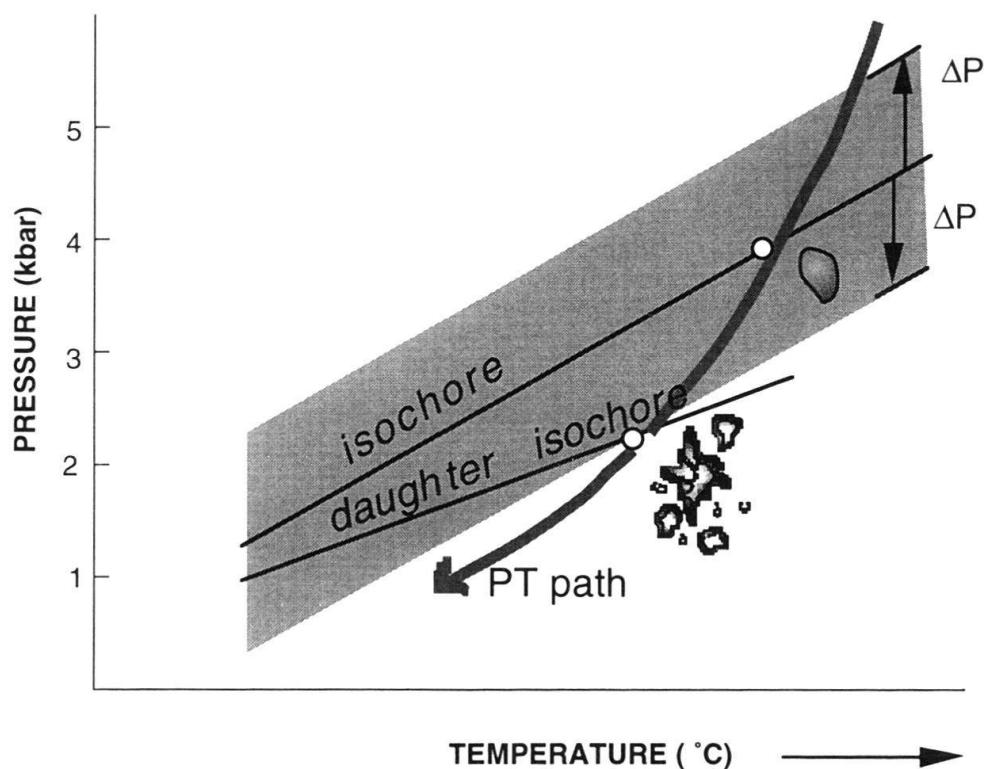


Fig. 9. Sketch illustrating the inclusion explosion process. This takes place when the difference between the internal fluid pressure of the inclusion (defined by the isochore) and the varying external confining pressures exceeds a critical value  $\Delta P$  (shaded bar). When this occurs, new daughter inclusions with densities corresponding to the surrounding pressure are formed. An isochore for the daughter inclusions is thus defined.

somewhere along its isochore. Since the P28-1 inclusions are not decrepitated, the P-T path segment following the trail formation must have been such that the difference between internal and external pressure never exceeded the critical overpressure  $\Delta P$  (shaded band in Fig. 8). Because of tectonic evidence (see below) we favour a roughly isobaric trajectory within this band. Cooling therefore occurred with very limited pressure decrease. On its way to lower P-T values our P-T-t path passed near the Al-silicate triple point. No andalusite is found in the Piona rocks, but in rocks a few kms higher in the crust (to the south in present day coordinates) the pressures were low enough to enter the andalusite field; cm-sized andalusite crystals in quartz nodules are reported in the Corenno Plinio region (Reposi 1914, El Tahlawi 1965, Mottana et al. 1990).

Our Rb-Sr data show that cooling through muscovite and feldspars closing temperatures occurred at 220–200 Ma. Preliminary  $^{40}\text{Ar}/^{39}\text{Ar}$  mica ages indicate that cooling continued and temperatures below ca. 350 °C were reached at 200–195 Ma (Wijbrans & Bertotti 1994). This is compatible with conventional K-Ar mica ages scattering between 250 and 190 Ma (Mottana et al. 1985).

During their last evolutionary stage the Piona schists experienced cooling and pressure decrease. Preliminary fission track data on zircons show that the Piona rocks were exhumed passing through the zircon annealing temperature (ca. 250 °C) at about 40 Ma

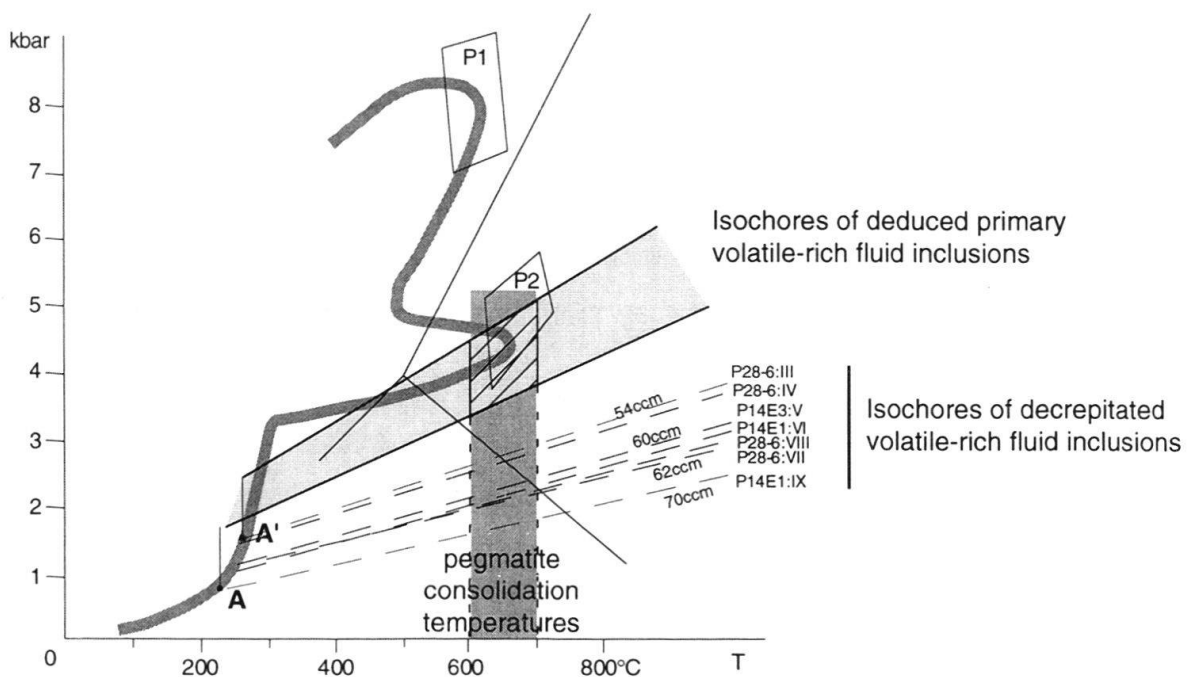


Fig. 10. P-T diagram showing the isochores determined for the Piona pegmatites (dashed lines) with the corresponding molar volumes in cubic centimetres (Holloway & Reese 1974; van den Kerkhof 1988) and the P-T path. The points A and A' mark the range of intersections of the daughter inclusion isochores with the P-T path derived for the country rocks. Adding the critical pressure of 1 kbar, the isochores of the parent inclusions are derived (thick solid lines); their intersections with the range of consolidation temperatures define the P-T box for pegmatite emplacement.

(data by D. Seward, pers. comm.). This is compatible with the isochores of the daughter inclusions. Decrepitation of the primary inclusions at temperatures below 200 °C is in general very unlikely because of the small difference between internal and external pressure. Furthermore, it would have produced completely different isochores of the primary and daughter inclusions not in accordance with the geologic history of the Piona section.

#### *The emplacement of the pegmatites*

Once the P-T path has been established, we can use the gaseous daughter inclusions (explosion products) to reconstruct the P-T conditions during pegmatite emplacement. In general, explosion occurs when the fluid pressure in fluid inclusions exceeds the confining pressure in the rock by a critical amount,  $\Delta P$ , which is a function of the type of host mineral and of the fluid inclusion size (Fig. 9). The critical overpressure for 20–40  $\mu\text{m}$  large fluid inclusions in quartz in the pegmatites is ca. 1 kbar (Roedder 1984). The external pressure at the moment of explosion is given by the intersection of the isochores of the daughter inclusions with the P-T path of the surrounding rock (values ranging between A and A' in Fig. 10). Adding the critical overpressure of 1 kbar to the daughter inclusions isochores, we derive a new set of isochores representative of the original primary inclusions (thick solid lines in Fig. 10). The new set gives a first constrain for the conditions during pegmatite emplacement. Assuming a consolidation temperature of 600–700 °C for

the pegmatites, the isochores predict an environment pressure of 3.5–5 kbar at the moment of emplacement (box in Fig. 10). These conditions overlap with the P-T estimates for the development of the P2 paragenesis, thereby confirming the syn-P2 emplacement of the pegmatites.

### **The tectonic evolution of the Lake Como section**

The first stage of deformation and metamorphism of the Piona rocks (Fig. 11) is clearly related to the Variscan orogeny which affected all basement units of the central-western Southern Alps (Siletto et al. 1993). Unfortunately, although the metamorphic conditions are fairly well constrained, very little is known about the structures associated with it. Folding in the Lake Como area probably occurred around NE-SW trending axes but further investigations are needed to obtain a clearer picture.

Our P-T-t path suggests that the Piona rocks were subsequently exhumed by at least 6–7 km. The structures which accommodated the exhumation and the driving forces of such movements are not known. The upward movement must have ended before the Late Permian when clastic sediments were deposited which seal older structures and show no abrupt thickness changes (Assereto & Casati 1965). Assuming that the exhumation lasted from 300 Ma (cooling below  $550 \pm 50$  °C) to 260 Ma (rough estimate for the onset of clastic sedimentation) we derive a minimum exhumation rate of 0.2 mm/yr. However, the exhumation could also have been accomplished earlier and more rapidly as suggested by amphibolite facies clasts in the sedimentary fill of Early Permian, roughly NE-SW elongated grabens (Cassinis et al. 1986) and by the limited occurrence of high-grade metamorphic clasts in the Upper Permian conglomerates (e.g. Gaetani et al. 1986). These observations suggest exhumation rates of the order of 1 mm/yr.

Evidence from the sedimentary record indicates that the upper crust of the central and western Southern Alps gently subsided from the late Permian until the Middle Triassic. Downward movement can be estimated at less than 2 km on the basis of sediment thickness. Vertical movements during the Carnian were more irregular, leading to substantial thickness variations across the Southern Alps. There is, however, no indication of major normal faulting (figure 2 in Brack & Rieber 1993). Thermal conditions in the lower crust and below were probably repeatedly perturbed by magmatic episodes during this same time span (e.g. Pinarelli et al. 1988, Gebauer 1993). Our new Rb-Sr absolute ages suggest that the thermal event which caused the formation of the pegmatites started at some time around ca. 240 Ma. This overlaps with intrusive events detected by Stähle et al. (1990) and, more relevant, with tuffitic horizons intercalated in the South-Alpine carbonate sequences (Jadoul & Rossi 1982, Mundil et al. 1995) which are related to strong volcanism in the subsurface of the present-day Po Plain (Brusca et al. 1981). We consider that the development of the P2 assemblage and the melting of meta-pelites at deep crustal levels to form the Piona pegmatites probably occurred during this event.

Whatever the duration and genesis of the thermal perturbations, generalized cooling of the South-Alpine crust was already taking place at 220–210 Ma and continued for most of the Jurassic (Fig. 11). The integrated cooling rates between the time that the Rb-Sr and the Ar-Ar blocking temperatures were reached range from 5.7 to 8.3 °C/Ma. While cooling was continuing, normal faulting along the E-dipping Lugano-Val Grande normal fault started at about 215–220 Ma (Bertotti 1991) marking the onset of rifting in the

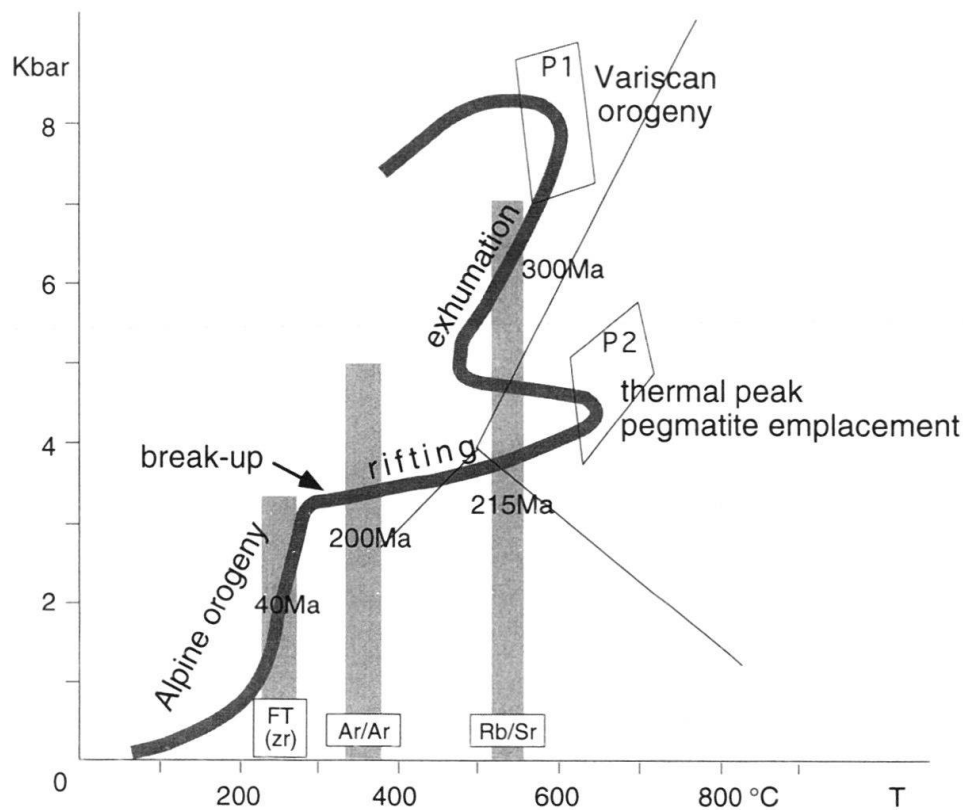


Fig. 11. P-T-t path for the tectonometamorphic evolution of the Piona crustal segment.

Southern Alps (Bertotti et al. 1993a). Our P-T-t path for the Piona rocks during this stage shows continued cooling under roughly isobaric conditions. Since the Piona rocks were part of the foot-wall of the Lugano-Val Grande normal fault and therefore remained in a very stable tectonic position (Bertotti 1991), the cooling shown by the P-T path suggests that ongoing rifting caused no major thermal anomaly (e.g. ter Voorde & Bertotti 1994, Bertotti & ter Voorde 1994). Extension ended in the Middle Jurassic with the formation of oceanic crust (Bertotti et al. 1993a).

The stable P-T pattern was finally perturbed by the onset of Alpine shortening which caused the pressure decrease and cooling. The cause and kinematics of the Tertiary exhumation and cooling (thrusting vs. isostasy) is still poorly known because of the lack of good control on the activation time of the various South-Alpine structures. Southward thrusting possibly started in the Late Cretaceous (Doglioni & Bosellini 1991) and probably ended in the Middle Miocene (Bernoulli et al. 1989).

## Conclusions

Following or overlapping with the last stages of Variscan shortening, parts of the South-Alpine crust, such as the Dervio-Olgiasca zone, have undergone important exhumation (Diella et al. 1992). The geological evidence suggests that the exhumation ended before the Late Permian and therefore cannot be directly related to the Late Triassic to Middle Jurassic rifting and passive margin formation. The tectonic context under which the exhu-

mation took place was one of continent-scale wrenching between Africa and Laurasia (Ziegler 1988) superimposed on post-orogenic instabilities of the Variscan mountain chain (Eisbacher et al. 1989, Malavieille 1993). It must be emphasized that the extension accommodated by the presently known grabens in the Southern Alps (Collio grabens) is far less than what needed to cause the amount of exhumation observed in the Dervio-Olgiasca zone. Similarly, very little is known about the existence of important Permian strike-slip faults and associated structures.

In the Middle Triassic, the relatively stable condition of the crust was brought to an end by a thermal event, possibly caused by important intrusions in the lower crust/upper mantle (Bertotti & ter Voorde 1994). The existence of the thermal anomaly has been previously proposed (e.g. Ferrara & Innocenti 1974), but its relevance was probably underestimated. We have documented in this paper the mineralogical changes which occurred due to the thermal event. Similar mineralogical changes have been described and similarly interpreted in the Austroalpine nappes of Tirol (Gregnanin & Piccirillo 1972). Fluids associated with the intrusion(s) were probably also responsible for some of the metallogenic events known from the Southern Alps which were previously tentatively related to the Early to Middle Permian magmatism (c.f. Cassinis et al. 1986). Furthermore, the intrusion(s) is likely to have caused vertical movements which, in their turn, must have affected the geometry of the Middle Triassic sedimentary bodies. We have not carried out numerical modelling to predict the extent of vertical movements but thickness differences in Middle Triassic sediments of several hundred metres are well known (c.f. Brack & Rieber 1993) and could well be related to these events.

The data presented in this paper establish that no major heating accompanied rifting and break-up in the South-Alpine continental crust, at least as deep as the middle crust. This is in accordance with numerical modelling results which underline the importance of conductive cooling during slow rifting (Bertotti & ter Voorde 1994, ter Voorde & Bertotti 1994). The cooling shown in our P-T-t path is related to the waning of a thermal anomaly that was emplaced shortly before the onset of normal faulting. It is tempting to speculate that the onset of normal faulting and extensional deformation was triggered by the intrusion and the related thermal anomaly rather than vice versa. This, obviously, leaves open the question of the origin of the intrusion.

### Acknowledgements

We thank J. Touret and P. Andriessen for the interesting discussion; we also thank the staff of the rock preparation and isotope labs and E. Burke for RAMAN analyses. J. Mullis (Basel) is thanked for his constructive review. A. Mottana is acknowledged for providing some publications. We also thank N. Froitzheim (Basel) for his assistance in the somewhat troubled review process. G.B. acknowledges financial support by AWON-GOA. This is publication n. 951101 of the Netherlands Research School on Sedimentary Geology.

### REFERENCES

- ASSERETO, R. & CASATI, P. 1965: Revisione della stratigrafia permo-triassica della Val Camonica meridionale (Lombardia). *Riv. ital. Paleont. Strat.* 71, 999–1097.
- BERNOULLI, D., BERTOTTI, G. & ZINGG, A. 1989: Northward thrusting of the Gonfolite Lombarda ("South-Alpine Molasse") onto the Mesozoic sequence of the Lombardian Alps: Implications for the deformation history of the Southern Alps. *Ecl. Geol. Helv.* 82, 841–856.

- BERTOTTI, G. 1990: The deep structure of the Monte Generoso basin: an extensional basin in the South-Alpine Mesozoic passive continental margin. *Mém. Soc. Géol. Fr.* 156, *Mém. Soc. Géol. Suisse* 1, *Mem. Soc. Geol. It.* 1, 303–308.
- 1991: Early Mesozoic extension and Alpine shortening in the western Southern Alps: the geology of the area between Lugano and Menaggio (Lombardy, Northern Italy). *Mem. Sc. Geol. (Padova)* 43, 17–123.
- BERTOTTI, G. & TER VOORDE, M. 1994: Thermal effects of normal faulting during rifted basin formation. 2: The Lugano-Val Grande normal fault and the role of pre-existing thermal anomalies. *Tectonophysics* 240, 145–157.
- BERTOTTI, G., PICOTTI, V., BERNOULLI, D. & CASTELLARIN, A. 1993a: From rifting to drifting: Tectonic evolution of the South-Alpine upper crust from the Triassic to the Early Cretaceous. *Sed. Geol.* 86, 53–76.
- BERTOTTI, G., SILETTO, G.B. & SPALLA, M.I. 1993b: Deformation and metamorphism associated with crustal rifting: the Permian to Liassic evolution of the Lake Lugano–Lake Como area (Southern Alps). *Tectonophysics* 226, 271–284.
- BOCCHIO, R., CRESPI, R., LIBORIO, G. & MOTTANA, A. 1980: Variazioni composizionali delle miche chiare nel metamorfismo progrado degli scisti sudalpini dell'alto Lago di Como. *Mem. Sc. Geol. (Padova)* 34, 153–176.
- BONIN, B. & 16 OTHERS 1993: Late Variscan magmatic evolution of the Alpine basement. In: *Pre-Mesozoic geology in the Alps* (Ed. by VON RAUMER, J.F. & NEUBAUER, F.), 171–201.
- BORIANI, A., DAL PIAZ, G.V., HUNZIKER, J.C. VON RAUMER, J. & SASSI, F.P. 1974: Caratteri, distribuzione ed età del metamorfismo prealpino nelle Alpi. *Mem. Soc. geol. ital.* 13 suppl. 1, 165–225.
- BRACK, P. & RIEBER, H. 1993: Towards a better definition of the Anisian/Ladinian boundary: new biostratigraphic data and correlations of boundary sections from the Southern Alps. *Ecl. Geol. Helv.* 86, 415–528.
- BRUSCA, C., GAETANI, M., JADOUL, F. & VIEL, G. 1981: Paleogeografia ladinico-carnica e metallogenese del Sudalpino. *Mem. Soc. geol. ital.* 22, 65–82.
- CASSINIS, G. AND 13 OTHERS 1986: Report on a structural and sedimentological analysis in the uranium province of the Orobic Alps, Italy. *Uranium* 2, 241–260.
- CERNY, P. 1982: Petrogenesis of granitic pegmatites. In: *Short course in granitic pegmatites in science and industry* (Ed. by CERNY, P.). *Min. Ass. Canada*, 405–450.
- DIELLA, V., SPALLA, M.I. & TUNESI, A. 1992: Contrasting thermomechanical evolutions in the Southalpine metamorphic basement of the Orobic Alps (Central Alps, Italy). *J. metam. Geol.* 10, 203–219.
- DOGLIONI, C. & BOSELLINI, A. 1989: Eoalpine and mesoalpine tectonics in the Southern Alps. *Geol. Rdsch.* 76, 735–754.
- DODSON, M.H. 1979: Theory of cooling ages. In: *Lectures in isotope geology* (Ed. by JAEGER, E. & HUNZIKER, J.C.), 194–202.
- ECHTLER, H.O. & MALAVIEILLE, J. 1990: Extensional tectonics, basement uplift and Stephano-Permian collapse basin in a late Variscan metamorphic core complex (Montagne Noire, Southern Massif Centrale). *Tectonophysics* 177, 125–138.
- EISBACHER, G.H., LÜSCHEN, E. & WICKERT, F. 1989: Crustal-scale thrusting and extension in the Hercynian Schwarzwald and Vosges, Central Europe. *Tectonics* 8, 1–21.
- EL TAHLAWI, M.R. 1965: *Geologie und Petrographie des Nordöstlichen Comerseegebietes (Provinz Como, Italien)*. PhD Thesis, ETH Zürich.
- FERRARA, G. & INNOCENTI, F. 1974: Radiometric age evidence of a Triassic thermal event in the Southern Alps. *Geol. Rdsch.* 63, 572–581.
- FUMASOLI, M.W. 1974: *Geologie des Gebietes nördlich und südlich der Jorio-Tonale Linie im Westen von Gravedona (Como, Italia)*. PhD Thesis, ETH Zürich.
- GAETANI, M., GIANOTTI, R., JADOUL, F., CIARAPICA, G., CIRILLI, S., LUALDI, A., PASSERI, L., PELLEGRINI, M. & TANNIOIA, G. 1986: Carbonifero superiore, Permiano e Triassico nell'area lariana. *Mem. Soc. geol. ital.* 32, 5–48.
- GAWEN, G.R.T., ROGERS, G., FALICK, A.E. & FARROW, C.M. 1995: Rb-Sr closure temperatures in bi-mineralic rocks: a mode effect and test for different diffusion models. *Chem. Geol.* 122, 227–240.
- GEBAUER, D. 1993: The pre-Alpine evolution of the continental crust of the Central Alps – An overview. In: *Pre-Mesozoic geology in the Alps* (Ed. by VON RAUMER, J.F. & NEUBAUER, F.), 93–117.
- GRADSTEIN, F.M., AGETRBERG, F.P., OGG, J.G., HARDENBOL, J., VAN VEEN, P., THIERRY, J. & HUANG, Z. 1994: A Mesozoic time scale. *J. Geophys. Res.* 99, 24.051–24.074.
- GREGNANIN, A. & PICCIRILLO, A.M. 1972: Litostratigrafia, tettonica e petrologia negli scisti austridici di alta e bassa pressione dell'area Passiria-Venosta (Alto Adige). *Mem. Ist. Geol. Min. Univ. Padova* 28, 2–55.

- HANSON, G.N., EL TAHLAWI, M.R. & WEBER, W. 1966: K-Ar and Rb-Sr ages of pegmatites in the south central Alps. *Earth Planet. Sc. Lett.* 1, 407–413.
- HOLDAWAY, J.M. 1971: Stability of andalusite and the aluminum silicate phase diagram. *Am. J. Sc.* 271, 97–131.
- HOLLOWAY, J.R. & REESE, R.L. 1974: The generation of N<sub>2</sub>-CO<sub>2</sub>-H<sub>2</sub>O fluids for use in hydrothermal experimentation: I. Experimental method and equilibrium calculations in the C-O-H-N system. *Am. Mineral.* 59, 587–597.
- JAHNS, R.H. 1982: Internal evolution of granitic pegmatites. In: *Short course in granitic pegmatites in science and industry* (Ed. by CERNY, P.). Mineral. Ass. Canada, 293–318.
- JADOU, F. & ROSSI, P.M. 1982: Evoluzione paleogeografico-strutturale e vulcanismo triassico nella Lombardia centro-occidentale. In: *Guida alla geologia del Sudalpino centro-occidentale* (Ed. by CASTELALRIN, A. & VAI, G.B.). *Guide Geol. Reg. Soc. geol. ital.*, 143–155.
- KERKHOF, A.M. VAN DEN 1988: The system CO<sub>2</sub>-CH<sub>4</sub>-N<sub>2</sub> in fluid inclusions: theoretical modelling and geological applications. PhD Thesis, Free University Amsterdam.
- MALAVIEILLE, J. 1993: Late orogenic extension in mountain belts: Insights from the Basin and Range and the Late Paleozoic Variscan Belt. *Tectonics* 12, 1115–1130.
- MGITANA, A., NICOLETTI, M., PETRUCCIANI, C., LIBORIO, G., DE CAPITANI, L. & BOCCHIO, R. 1985: Pre-Alpine and Alpine evolution of the South Alpine basement of the Orobic Alps. *Geol. Rdsch.* 74, 353–366.
- MOTTANA, A., CRESPI, R. & LIBORIO, G. 1990: The occurrence of three aluminosilicates at Corenno Plinio (Upper Lake Como region, Italy). *Mem. Sc. Geol. (Padova)* 42, 361–379.
- MUNDIL, R., BRACK, P., MEIER, M. & OBERLI, F. 1995: Calibration of Triassic “Milankovitch cycles” by high resolution U-Pb age determination. *Terra Nova* 7 suppl. 1, 351.
- PINARELLI, L., DEL MORO, A. & BORIANI, A. 1988: Rb-Sr geochronology of Lower Permian plutonism in Massiccio dei Laghi, Southern Alps (NW Italy). *Rend. Soc. ital. Min. Petr.* 43, 411–428.
- REPOSSI, E. 1914: I filoni pegmatitici di Olgasca. *Atti Soc. ital. Sci. Nat.* 52, 487–513.
- ROEDDER, E. 1984: Fluid Inclusions. *Reviews in mineralogy*, Min. Soc. Am. 12.
- SILETTO, G.B., SPALLA, M.I., TUNESI, A., NARDO, M. & SOLDI, L. 1990: Structural analyses in the Lario Basement (central Southern Alps, Italy). *Mem. Soc. geol. ital.* 45, 93–100.
- SILETTO, G.B., SPALLA, M.I., TUNESI, A., LARDEAUX, J.M. & COLOMBO, A. 1993: Pre-Alpine structural and metamorphic histories in the Orobic Southern Alps, Italy. In: *Pre-Mesozoic geology in the Alps* (Ed. by VON RAUMER, J.F. & NEUBAUER, F.), 585–598.
- STÄHLE, V., FRENZEL, G., KOBER, B., MICHARD, A., PUCHELT, H. & SCHNEIDER, W. 1990: Zircon syenite pegmatite in the Finero peridotite (Ivrea zone): evidence for a syenite from a mantle source. *Earth Plan. Sc. Lett.* 101, 196–205.
- THIERY, R., VAN DEN KERKHOF, A.F. & DUBESSY, J. 1994: vX properties of CH<sub>4</sub>-CO<sub>2</sub> and CO<sub>2</sub>-N<sub>2</sub> fluid inclusions: modelling for < 31 °C and P < 400 bars. *Eur. J. Min.* 6, 753–771.
- THOMPSON, A.B.T. & TRACY, R.J. 1979: Model systems for anatexis of pelitic rocks II. Facies series melting reactions in the system CaO-KAlO<sub>2</sub>-NaAl<sub>2</sub>O<sub>3</sub>-SiO<sub>2</sub>-H<sub>2</sub>O. *Contr. Min. Petrol.* 70, 429–438.
- VON BLANCKENBURG, F., VILLA, I.M., BAUR, H., MORTEANI, G. & STEIGER, R.H. 1989: Time calibration of a PT-path from the Western Tauern Window, Eastern Alps: the problem of closure temperatures. *Contr. Min. Petrol.* 101, 1–11.
- VOORDE, M. TER & BERTOTTI, G. 1994: Thermal effects of crustal normal faulting during rifted basin formation. 1: a finite difference model. *Tectonophysics* 240, 133–144.
- WIJBRANS, J.R. & BERTOTTI, G. 1994: Thermal evolution of the South-Alpine crust: from Variscan cooling to Alpine overprinting. 8th Int. Conf. Geochronology, Cosmochronology and Isotope Geology, Berkeley, June 5–11, 1994, abstract volume, 353.
- WILSON, M. 1993: Magmatism and geodynamics of basin formation. *Tectonophysics* 86, 5–29.
- YARDLEY, B.W.D. 1977: The nature and significance of the mechanism of sillimanite growth in the Connemara Schists, Ireland. *Contr. Min. Petrol.* 65, 53–58.
- ZIEGLER, P. 1988: Evolution of the Arctic-North Atlantic and the Western Tethys. *Amer. Assoc. Petrol. Geol. Mem.* 43, 1–197.

Manuscript received March 8, 1995

Revision accepted November 8, 1995

